Graft-Copolyamide Molecular Composites

SHAUL M. AHARONI

AlliedSignal Inc. Research and Technology, P.O. Box 1021, Morristown, New Jersey 07962

SYNOPSIS

A novel family of graft-copolyamides was prepared in which several chains of high molecular weight polycaproamide (nylon 6) are grafted onto the backbone of each stiff aromatic polyamide chain. The unique feature of the present graft-copolyamides is that the side chains are connected through amide groups directly to the aromatic rings in the stiff chain, and not to the amide groups in the backbone of the stiff chain. Because they are miscible with linear nylon 6, blends of the graft-copolymers and nylon 6 are easily prepared. Electron microscopy, x-ray diffraction scans, DSC runs, and solid-state NMR relaxation and spin diffusion experiments all indicate that the aromatic stiff polyamide chains are molecularly dispersed in the graft-copolyamides and their blends with nylon 6. In an ungrafted blend of the stiff aromatic and flexible aliphatic nylon 6, the stiff chains tend to agglomerate into small hydrogen-bonded sheaf-like aggregates the size of which increases upon annealing above the melting point of the flexible polyamide. The NMR results point to a substantial flexibility of the stiff chains in the graft-copolyamides, helping to explain the levels of reinforcement reflected in the tensile properties of these materials. In the ungrafted blends, the aromatic-chain stiffness is greatly enhanced when these chains are phase separated in the minute sheaf-like particles. The tensile properties of the graft-copolymers and their mixtures with pure nylon 6 are far superior to those of the ungrafted blends. The reinforcement of the flexible matrix by the stiff polyamide chains is explained in terms of the Halpin–Tsai formulation. © 1994 John Wiley & Sons, Inc.

INTRODUCTION

Stiff worm-like polymers that form lyotropic and thermotropic liquid crystals are known to have very high tensile modulus and strength in the chain direction.[1] This has led to many attempts to use them as reinforcement for flexible polymers. With very few exceptions, the stiff polymers were blended into the flexible polymers by either melt-blending or coprecipitation from a mutual solvent. As a rule, such blends show phase separation on nanometer or coarser scale. The separating stiff-chain macromolecules usually align themselves more or less parallel in small domains. In the presence of shear forces or during elongational deformations, these domains coalesce to form larger fibrillar structures. The phase separation and parallel alignment are driven by the strongly anisotropic shape and large axial ratio of the stiff-chain polymers, by the large difference in the entropy of stiff and flexible chains,[2,3] and by their chemical dissimilarity reflected by the magnitude of the difference between their solubility parameters.[4-7] Therefore, even when well-blended in a matrix of flexible chains, the worm-like molecules prefer to phase separate out of the flexible polymer and aggregate separately as pure stiff-chain agglomerates. Rapid quenching of the system may arrest such phase separation, but reheating to the melt regime of the flexible polymer, say, during melt processing, allows the phase separation process to continue and the average size of the minor phase to grow. Furthermore, practically as a rule, the bonding between the flexible chain matrix and the stiff-chain inclusions is very poor and strong interphase delamination is usually evident. This is due to several reasons. The most important among them are: the tendency to phase separate due to shape anisotropy; the incompatibility of the two phases due to substantial difference in their surface tension;[8] and the

difference in the shrinkage of the two phases upon cooling from the melt. The literature is replete with electron microscopy studies of the above, attempting to explain the rather disappointing mechanical properties of such blends. Examples are given in the references[9-20] of such work pertaining to blends of flexible polyamides with stiff worm-like polymers that often form liquid crystalline phases. Various chemical approaches were taken in order to improve the adhesion between the flexible polymer matrix and the stiff-chain inclusions. In the case of aromatic polyamide inclusions, these approaches involve the formation of ABA-type block copolymers,[9,19] substitution of the amide hydrogen by other groups which may or may not be further reacted,[11,21-26] and random attacks on the surface of polyamide micro-fibriles.[27-29] In this junction it is worth mentioning that several undefined and uncharacterized networks containing stiff polyamide segments were claimed in the literature.[30,31]

Some of the above authors maintain that infrared (IR) scans reveal the partial miscibility of aliphatic polyamides with fully aromatic polyamides, while at the very same time phase separations were observed to take place in the very same blends.[14,15,17] Other workers simply state that in similar blends they observe clear phase separation on a rather large scale.[9,16] No complete miscibility of flexible, fully aliphatic with stiff, fully aromatic polyamides was ever observed.

When all or some of the flexible polymer chains are grafted onto the backbones of the stiff worm-like polymer, the latter cannot phase separate out of the flexible polymer matrix. A schematic description of this is shown in Figure 1. An apparently successful procedure to arrest the phase separation of poly(p-phenylene terephthalamide)(Pp-PT) and nylon 3 was reported by Moore and Mathias.[32] Accordingly, the amide groups in Pp-PT are converted to the anionic form by reacting them with sodium hydride in dimethylsulfoxide.[21] In a subsequent step, acrylamide is first grafted onto the anionic sites on the Pp-PT backbone and then continuously polymerized by anionic initiation to form graft copolymer in which the backbone is aromatic and the side chains are flexible nylon 3. Together with the graft copolymer, substantial amounts of linear nylon 3 homopolymer are also produced. At Pp-PT concentrations higher than 30%, Pp-PT separates out of the blend in the form of coarse fibriles.[32]

In this article we report a novel method of creating polyamide molecular composites by synthesizing graft-copolymers with stiff aromatic polyamide chains as backbones and high molecular weight (high-M) polycaproamide (nylon 6) as the flexible side chains. *The unique feature of the present graft-copolyamides is that the side chains are connected, through amide groups, directly to the aromatic rings in the worm-like chains, and not to the amide groups present in the stiff backbones.* Results of sev-
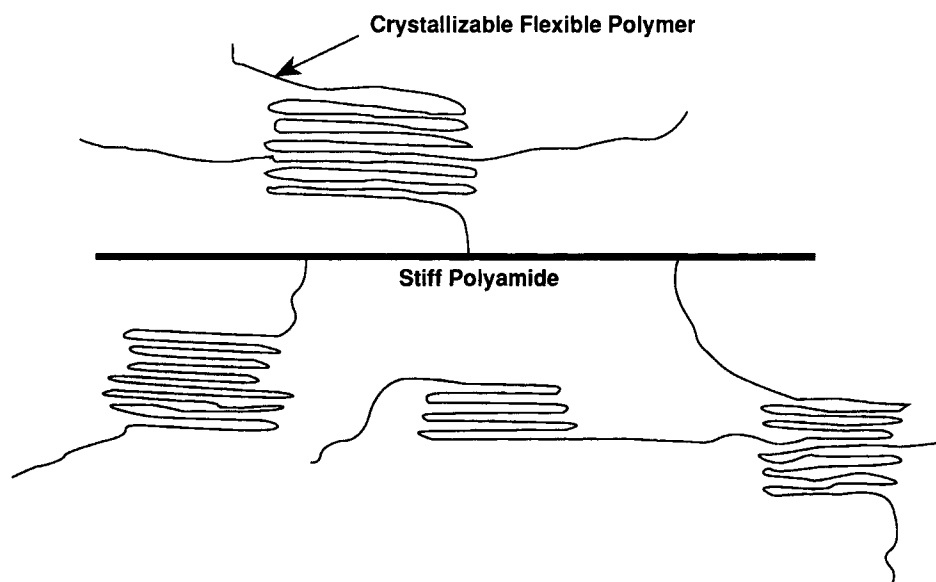
Figure 1   Schematic description of graft-copolymer present in the solid state together with co-crystallizable flexible polymer.

eral characterization studies and some mechanical properties will also be presented, demonstrating that the systems created in this work are indeed polyamide molecular composites. The technique of solid-state NMR ^{1}H spin diffusion was found to be an especially powerful tool in determining domain size[33,34] and, in our case, demonstrating the absence of separate aliphatic and aromatic amorphous phases in the grafted materials and their presence in the ungrafted blends. This technique is particularly useful in size scales too fine to discern by other techniques.[33,34]

EXPERIMENTAL

Synthesis, Grafting, and Blending

All monomers, reagents, and solvents were obtained from chemical supply houses in the highest available purity and used as received.

Two stiff-chain amine-carrying aromatic polyamides were prepared in two steps by first employing the Yamazaki procedure[35,36] to create nitro-bearing polymers and then reducing them to the amine groups. The Yamazaki polycondensation was carried in solution in N,N-dimethylacetamide (DMAc) containing 5 wt/vol % dry LiCl, using triphenylphosphite (TPP), and pyridine as reagents. The reaction was conducted at around 110°C and was allowed to proceed for 4 h after the addition of TPP. The polymeric products were then precipitated in a large excess of methanol and purified by repeated washing in methanol, room-temperature water, boiling water, and again in methanol. The polymers were then dried under vacuum at ca. 125°C and readied for the next reaction. We first used equimolar amounts of 4,4'-diaminobenzanilide (DABA) and nitroterephthalic acid (NTPA) to prepare the polymer:[37,38]
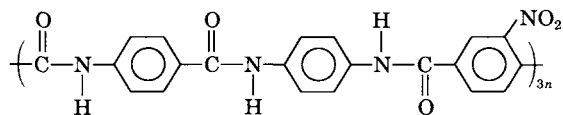
After workup and purification, this polymer was converted into the amine analogue by hydrogenation with either $SnCl_2 \cdot 2H_2O$/HCl mixture or a basic aqueous solution of sodium hydrosulfite ($Na_2S_2O_4$). Both procedures resulted in about $\frac{1}{3}$ of the nitro groups being reduced to amine. The resulting polymer (coded 25A) looks like:

25A
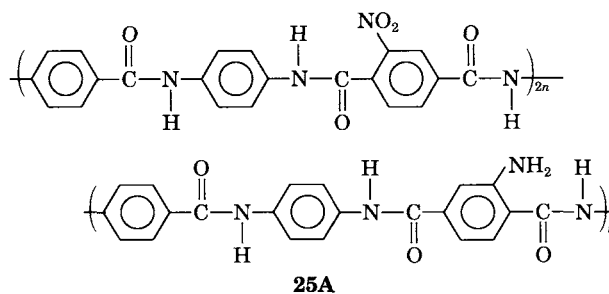
The second amine-bearing stiff polyamide (coded 50A3), was obtained in identical two steps from a 2 : 1 : 1 molar ratio mixture of the monomers DABA/NTPA/terephthalic acid (TPA). In this case, the average distance between substituted rings is about six rings and the distance between amine groups is about twice as large as in 25A:

50A3
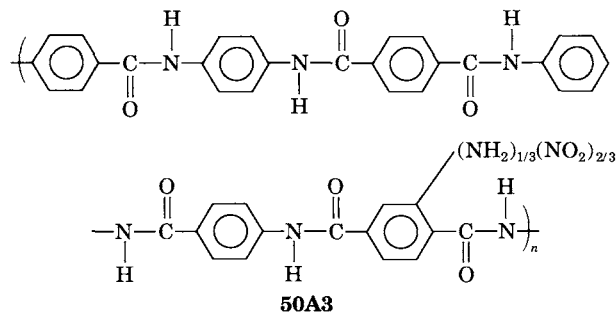
For the purpose of grafting a commercial grade of nylon 6 was used, having a weight average molecular weight M_w of 33,000 and a molecular weight distribution M_w/M_n of 3.0. This particular grade was selected because the large majority of the nylon 6 chains in it are terminated by a carboxyl group (A) on one end and an amine group (B) on the other. Such an AB-termination, that reduces the number of AA- and BB-chains to a very small minority, prevents the cross-linking and gelation of the system during grafting. Therefore, the grafting procedure described herein may be broadened to all AB-terminated flexible polyamides. This makes the grafting procedure useful for all AB-terminated nylon X and makes it impossible to graft common nylon XY (X and Y are positive integers) because the latter contains about 25% of the chains terminated with AA-ends and another 25% terminated with BB-ends.

Our preferred grafting method requires the separate dissolution of the stiff polyamide and the nylon 6 in DMAc/5% LiCl, each at concentrations of 3–7 wt/vol %. The dissolution temperature of the stiff

polyamide was 100–110°C and that of the nylon 6 higher. The smaller volume solution was then added to the larger volume one, followed by the addition of pyridine and TPP in slight molar excess. The condensation reaction was then allowed to continue at ca. 115°C with constant stirring for not less than 4 h. The polymeric products were then precipitated in a large excess of methanol, carefully washed as above, and finally dried to constant weight.

Blends of the grafted copolymers with pure nylon 6 were prepared by separately dissolving the two polymers in conc. H_2SO_4 at room temperature or in DMAc/5% LiCl at 135°C and then mixing the solutions. For the preparation of blends solutions of 5–6% were used. In each case the mixed solution was stirred for at least 1 h to effect thorough mixing and then poured in a thin stream into an intensively stirred mixture of ice and water in the case of H_2SO_4 or into methanol in the case of DMAc/5% LiCl. The solids were then filtered, passed through the blender, washed several times in cold and then boiling water, a few times in methanol, and finally dried under dynamic vacuum at up to 150°C. For the purpose of comparison, the pure nylon 6 and pure graft-copolymer were subjected to the same dissolution, precipitation, and work-up procedures as the blends.

Characterization

The structure of the stiff aromatic polyamides was verified by means of proton and ^{13}C NMR spectroscopy, performed in a 400 MHz Varian XL-400 spectrometer on solutions of the polymers in deuterated solvents such as d_6-DMAc and D_2SO_4. To estimate the grafting efficiency of the aliphatic nylon 6 onto the aromatic stiff polyamides, the reaction products were fractionated by exhaustive extraction at room temperature with 2,2,2-trifluoroethanol (TFE), which is a good solvent for nylon 6 and a nonsolvent for the grafted material. Mass-balance analysis was performed on the starting polymers, on the TFE-insoluble and on the TFE-soluble fractions. The amounts of aromatic and aliphatic residues in the starting materials and the two fractions were further estimated from integration of the relevant resonances in NMR scans performed on their solutions in D_2SO_4 and from the relative intensities of the appropriate absorption bands in IR spectra. These were obtained from the samples pulverized in KBr matrix, using a Perkin–Elmer 983 ratio-recording double-beam dispersive IR spectrophotometer. The concentrations of aliphatic and aromatic polyamides were estimated from computer-calculated absorbance differences between the samples and appro-

priate blanks. The same IR instrument and procedure were used to estimate the efficiency of reduction of the nitro groups to amines during the preparation of the stiff polyamides 25A and 50A3.

Solid-state NMR experiments were performed on samples molded in the melt and quick quenched (QQ) to room temperature. The samples were then equilibrated for about 3 months in 50% relative humidity atmosphere before being studied in the NMR instrument. Solid-state NMR ^1H spin diffusion rate measurements were used to characterize domain size in the graft-copolymer samples, in blends of graft-copolymers with pure nylon 6, and in ungrafted blends of the stiff polyamides and nylon 6.[39] $T_{1\rho H}$ measurements aided in locating the position of the grafted stiff polyamides in the nylon 6 matrix, and T_{1H} measurements gave an estimate of the distances between the stiff aromatic chains and the crystalline nylon 6 domains. All solid-state NMR experiments were performed in a Chemagnetics CMX-300 instrument, operating at 300 MHz for ^1H and 75 MHz for ^{13}C. The temperature was maintained at 25°C. The magic angle was adjusted with KBr, and all samples were spun at near 4 kHz. The solid-state NMR results were obtained[40] using seven different pulse sequences. The experimental details and specific pulse sequences are described in detail in the literature[33,34,39] and in a forthcoming paper.[40] The various phases of nylon 6 and of nylon 6 in the graft-copolymers were studied by the use of the following three procedures: cross-polarized magic angle spinning (CPMAS); short contact times and exact Hartmann–Hahn match to obtain the selective spectrum of crystalline nylon 6; and Bloch decay (BD) sequences to obtain the selective spectrum of amorphous nylon 6. Details and explanations of the above NMR procedures can be found in the references.[33,34,39–48]

Thermal scans were obtained from samples in nitrogen atmosphere using a DuPont 9900 DSC (differential scanning calorimetry) instrument operating at 20 K/min heating and cooling rate. Between the heating and cooling cycles each sample was kept for at least 2 min at 270°C or higher.

Wide-angle x-ray diffraction (WAXD) patterns were obtained in a Philips APD-3600 automatic diffractometer operating in parafocus mode using copper radiation and a diffracted beam monochromator. Optical microscopy studies at 100× magnification were conducted with an Olympus BH-2 polarized-light microscope equipped with a Mettler FP-82 hot stage and controlled by a Mettler FP-80 central processor. Samples for transmission electron microscopy (TEM) were cryosectioned at temperatures

close to $-60°C$ and examined in a Hitachi H-800 electron microscope. Although initially stained by phosphotungstic acid, it was found that staining was not necessary due to the large difference in the densities of the aromatic and aliphatic polyamides. The results of stained and unstained samples turned out to be essentially the same. All original micrographs were printed at a magnification of 71,000×.

To prepare tensile test specimens, the powdered polymers were compression molded into plaques not thinner than 1.0 mm, and then QQ to room temperature in a crushed ice/water mixture. Specimens conforming with ASTM procedure D638 were later punched out and allowed to reach equilibrium at 50% relative humidity (RH), a process that took up to 3 months. The equilibration process was followed by weighing all test specimens daily. The tensile properties of the QQ and equilibrated specimens were measured in a computer-controlled Instron machine model TTD using a 0.5 in/min head speed and following the ASTM D638 procedure.

Dilute solution viscosities were measured at 25°C on solutions of the polymers in concentrated sulfuric acid using internal dilution Cannon–Ubbelohde glass viscometers with solvent efflux times longer than 100 s.

RESULTS AND DISCUSSION

Fractionation of the graft-copolymerization products followed by mass-balance, IR analysis, and NMR scans obtained from the fractions soluble and insoluble in TFE, revealed that the grafting effi-

ciency was over 85% for both stiff aromatic polyamides. This high efficiency is most likely caused by the preponderance of amine groups pendant to the stiff aromatic chains and the relatively low concentration of amine ends of the flexible nylon 6. Increasing concentration of nylon 6 amine and carboxy chain ends will gradually shift the equilibrium toward larger fraction of nylon 6 chain extension and a smaller fraction of graft-copolymer. Intrinsic viscosity results of the stiff aromatic polyamides, nylon 6, their graft-copolymers, blend, and blends of graft-copolymer with nylon 6, are all shown in Table I. The fact that the intrinsic viscosity of the graft-copolymers is consistently higher than that of the precursor polymers and of the ungrafted blend, indicates that grafting indeed took place. Using the relationship

$$[\eta] = 5.93 \times 10^{-5} M_w^{1.068}$$

previously obtained[38] from light scattering and viscosity measurements, we find for the stiff polyamide 50A3 an M_w a little higher than 6800. Recalling that only one ring out of six in 50A3 is nitrated and that the reduction to amine was only about 35% efficient, we conclude that in each 50A3 chain there exist on the average only one or two reactive amine groups and only one or two nylon 6 chains were grafted on it. This is the reason why the intrinsic viscosity of the graft-copolymers in series 58 is only slightly higher than that of pure nylon 6. In the case of polyamide 25A the concentration of amine groups along the stiff chain is at least twice as high as in 50A3. This results in a substantially higher level of grafting

Table I Intrinsic Viscosity and Thermal Transitions of Polymers

Code	Description	$[\eta]$ (dL/g)	T_g (°C)	T_m (°C)	ΔH_m (J/g)	T_{cc} (°C)	ΔH_{cc} (J/g)
49-1	Graft-copolymer of 85% N6 on 15% 25A	2.10	67.9	215.6	36.9	161.8	37.4
49-2	Blend of 49-1 and 49-5 giving 88/12, N6/25A	2.00	65.0	218.2	31.5	171.6	36.6
49-3	Blend of 49-1 and 49-5 giving 92/08, N6/25A	1.90	64.2	218.0	31.5	176.2	34.6
49-4	Blend of 49-1 and 49-5 giving 96/04, N6/25A	1.85	62.0	222.5	36.2	178.4	38.8
49-5	N6 (LSL grade) used in series 49	1.27	56.0	224.1	47.1	179.4	53.5
49-6	Blend of 85% N6 and 15% 25A, no grafts	1.10	67.0	209.2	23.5	171.2	25.5
58-1	Graft-copolymer of 85% N6 on 15% 50A3	1.31	51.8	217.9	—	168.0	—
58-2	Blend of 58-1 and 58-5 giving 88/12, N6/50A3	1.32	50.2	219.0	—	169.6	—
58-3	Blend of 58-1 and 58-5 giving 92/08, N6/50A3	1.33	48.6	219.8	—	170.7	—
58-4	Blend of 58-1 and 58-5 giving 96/04, N6/50A3	1.31	47.7	220.5	—	172.0	—
58-5	N6 used in series 58	1.21	45.5	222.0	—	175.4	—
25A	Stiff polyamide used in series 49	0.68	No visible transitions up to 350°C				
50A3	Stiff polyamide used in series 58	0.74	No visible transitions up to 350°C				

N6, nylon 6.

on 25A, reflected in intrinsic viscosity of 49-1 significantly higher than 58-1.

As can be seen from Table I, the stiff polyamides failed to show any glass-transition temperature, T_g, or melting point, T_m, up to the onset of thermal degradation at about 350°C. Grafting increases the T_g of the nylon 6 component in graft-copolymers and, at the same time, decreases the T_m and T_{cc} (crystallization temperature upon cooling from the melt) of the nylon 6 component. When the graft-copolymer is thoroughly mixed with pure nylon 6, the values of T_g, T_m, and T_{cc} gradually shift from their values for pure nylon 6 to their values in the graft-copolymers 49-1 and 58-1, respectively. It will be shown below that the percent crystallinity of the pure nylon 6 and its graft-copolymer remains about the same. Therefore, the reduction in T_m and T_{cc} cannot be ascribed exclusively to lower crystallinity but may be associated, at least in part, with highly defective crystallites of decreasing size. The modest increases in T_g may be ascribed to reduction in chain mobility of the grafted nylon 6. This reduced chain mobility is probably a contributing cause to the nylon 6 crystallites increasing disorder and diminishing size upon grafting. It is not unexpected but important to note that no indication was found in any of the thermal scans for the presence of a separate phase of the stiff polyamides in the graft-copolymers.

Heats of melting and crystallization were obtained only for series 49. They clearly indicate that the heats of pure nylon 6, sample 49-5, are higher than any of the corresponding heats of the graft-copolymer 49-1 and the blends containing the graft-copolymer, samples 49-2 through 49-4. The lower heats of transition may reflect any of: (a) reduced total crystallinity, (b) reduced crystallites size, (c) increased disorder within the crystalline phase. We believe that in our case, reasons (b) and (c) are the more important ones.

The blend 49-6, containing no grafted material, poses some difficulties. Its T_g and T_m are as high as those of the graft-copolymer 49-1, and its T_{cc} is somewhat higher. On the other hand, the heats of both T_m and T_{cc} are far below any of the other members of series 49. We are not certain of the reasons for this, but an educated guess is that upon cooling from the melt, the presence of the stiff polyamide 25A in very small aggregates in the nylon 6 matrix interferes only modestly with the average chain mobility of the nylon. Thus T_{cc} happens about halfway between pure nylon 6 and the graft-copolymer 49-1. The size of the growing crystallites and their perfection are adversely affected by the presence of the stiff second phase, hence the low heat of crystallization. Upon heating from the glassy state the situation is different. Here, chain mobility in the glassy phase is limited to start with. The presence of minute particles of a stiff second phase further inhibits chain mobility, demanding higher temperature for the onset of the glass transition than pure nylon 6. The temperature and heat of transition of the melting point are, of course, dictated by the crystallization that preceded the melting, in our case T_{cc}. Thus, the high T_g, low T_m, and intermediate T_{cc} are all prescribed by varying measures of inhibition of the mobility of nylon 6 chains. In the case of graft-copolymer 49-1 the mobility restrictions are permanent in nature and independent of whether we are in the glassy or molten states, and hence the high T_g and low T_m and T_{cc}.

WAXD patterns of the as-prepared dry samples 49-1 through 49-6 were inconclusive and showed the presence of about 50% crystallinity in all of them. The WAXD patterns were those of nylon 6 alone with no indication of the presence of another phase in the graft-copolymer 49-1 and the blends 49-2, 49-3, and 49-4, and the ungrafted blend 49-6. However, because the WAXD patterns of linear stiff aromatic polyamides are so similar to that of nylon 6,[38] our inability to detect the presence of aggregates of such stiff polyamides is not unexpected. With respect to the observed crystallinity, in all cases about 65% of the crystal phase were in the α-form of crystalline nylon 6, and about 35% in the γ-form. There was a very small increase in the relative weight of α vs. γ upon going from the graft-copolyamide 49-1 toward the pure nylon 49-5. The blend 49-6 was about halfway in between. However, because the total range of the α and γ forms was within 5% from 65 and 35%, respectively, these small changes in α and γ crystallinities are not significant.

As was the case with the DSC and WAXD scans, hot-stage polarized light microscopy failed to show any phase separation in the graft-copolymers. Studies were conducted on the graft-copolymer 49-1, on the ungrafted blend 49-6, and on the pure nylon 6 49-5. In all cases the polymers were heated on the hot-stage at 10 K/min to a predetermined temperature and after equilibration for at least 10 min, their response to mechanical stresses was tested by applying pressure and shear to the microscope cover-glass. The samples were then allowed to relax once more and then studied in polarized and unpolarized light to detect phase separation. All three samples showed fine-grained birefringence at ambient temperature. The pure nylon sample 49-5 softened and lost its birefringence at the lowest temperature of the three, about 218°C. It became fully extinguishing

and highly fluid at 227°C. The graft-copolymer 49-1 maintained its birefringence and remained stiff up to 280°C even after subsequent equilibration steps at 240, 250, and 260°C. No phase separation was visible up to and including 280°C. After residence of about 15 min at 280°C the material started uniformly losing its birefringence. When studied by means of unpolarized light, the material showed some discoloration typically associated with the onset of thermal degradation. The ungrafted blend 49-6 showed a different behavior. Here, the system started moderately birefringent. Upon equilibration at 250°C for only 5 min, 49-6 lost all its birefringence. In thin sections of the sample phase separation became clearly evident during the 250°C equilibration. Despite the loss of birefringence, 49-6 remained rather stiff up to 280°C. From the above it is obvious that while the graft-copolymer remained homogeneous until thermal degradation sets in, a phase separation takes place in the ungrafted blend already at 250°C. The biphasic system maintains,

however, a very high melt viscosity up to about 280°C. Melt viscosity studies, not reported here, were found to be fully consistent with the observations on the microscope hot stage.

TEM was performed on cryosectioned samples of the graft-copolymers 49-1, 58-1, on the ungrafted blend 49-6, and on blends of nylon 6 with 49-1. The blends of nylon 6 with 49-1 appeared identical to 49-1 and will not be discussed further. The photomicrograph shown in Figure 2 of sample 49-1 is typical of all other areas of samples 49-1 and 58-1 observed on the microscope CRT screen. In all these instances, the samples appeared rather featureless. The stiff aromatic polyamide is invisible in all of them. In Figure 3 the ungrafted blend 49-6 is shown. It contains the same 15% concentration of stiff polyamide chains as 49-1 and 58-1. Unlike these, in 49-6 a phase separation is clearly evident with the stiff aromatic polyamide aggregates standing out as dark inclusions. A careful observation of these inclusions reveals the preponderance of elongated in-
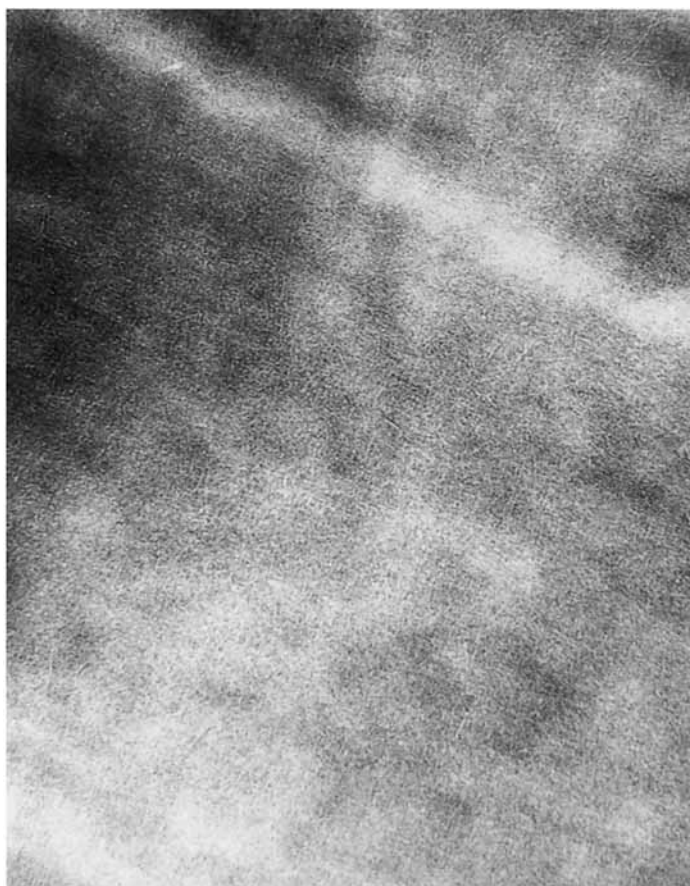
**Figure 2**   Typical micrograph of the graft-copolymer 49-1. Original magnification: 71,000×.
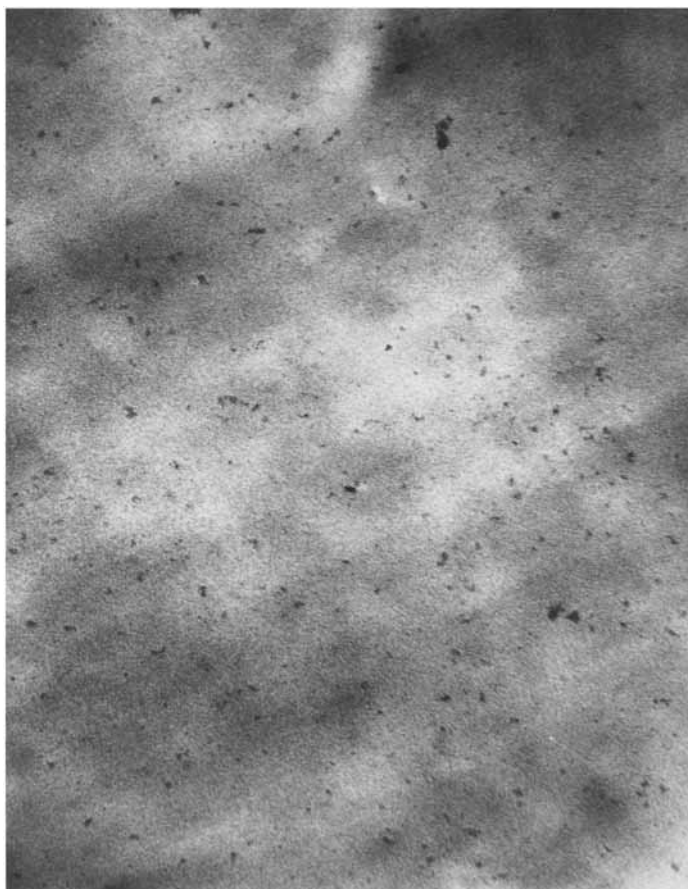
Figure 3 Typical micrograph of the ungrafted blend 49-6. Original magnification: 71,000×.

clusions randomly oriented in space. Assuming the aggregates are cylindrical in shape, the smallest diameter observed was in the 25–30 Å range. This corresponds to aggregates of 20 or more stiff chains existing in sheaf-like entities. In all the above, the results of stained and unstained samples were identical. From the above we conclude that the grafting of nylon 6 onto stiff aromatic polyamide chains prevents these from aggregating together in solution or in the melt. When the nylon is not grafted onto the stiff chains, these do aggregate into a separate phase given sufficient time in solution or when the nylon is in its molten state.

Solid-state NMR spin diffusion experiments[34] are especially adept at determining the smallest dimensions of coexisting phases. Typical T_{1H} relaxation plots for crystalline nylon 6 and stiff polyamide 25A used in the graft 49-1 and blend 49-6 are shown, respectively, in Figures 4 and 5. Spin diffusion times in the graft-copolyamide 49-1 and the ungrafted blend 49-6 are shown in Figures 6 and 7, respectively. These and other spin diffusion experiments not

shown here,[40] together with the relaxation experiments, have shown that: First, in all graft-copolymers the stiff macromolecules are characterized by the smallest domain size of 5–10 Å, corresponding to the diameter of a single stiff chain. The stiff chains are, hence, individually dispersed in the nylon 6 matrix of the graft-copolymer. Second, in ungrafted blends the smallest domain size of the stiff polyamide is 10–20 Å. This means that the stiff chains tend to agglomerate in small sheaf-like aggregates, each containing about 10 stiff chains. Third, the stiff aromatic chains in the graft-copolymers are preferentially dispersed in the amorphous fraction of the nylon matrix. Fourth, the average size of the amorphous and crystalline phases in the nylon 6 matrix are both of the order of 100 Å. Fifth, in the graft-copolymers, the individual stiff polyamide chains show rapid relaxation, that is, higher flexibility. When aggregated in the ungrafted blend they show slow relaxation, that is, higher rigidity. This higher rigidity is probably caused by interchain H-bonding in the sheaf-like aggregates. The higher flexibility
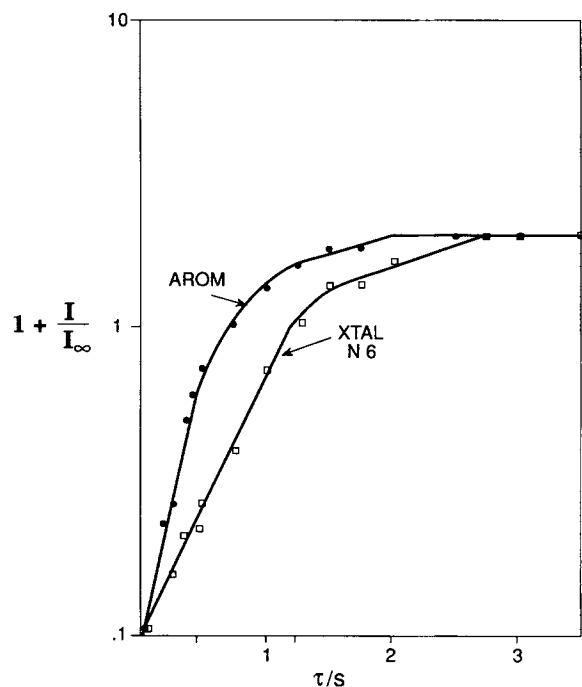
Figure 4 T_{1H} relaxation plot of crystalline nylon 6 and the stiff aromatic polyamide 25A present in the graft-co-polymer 49-1.
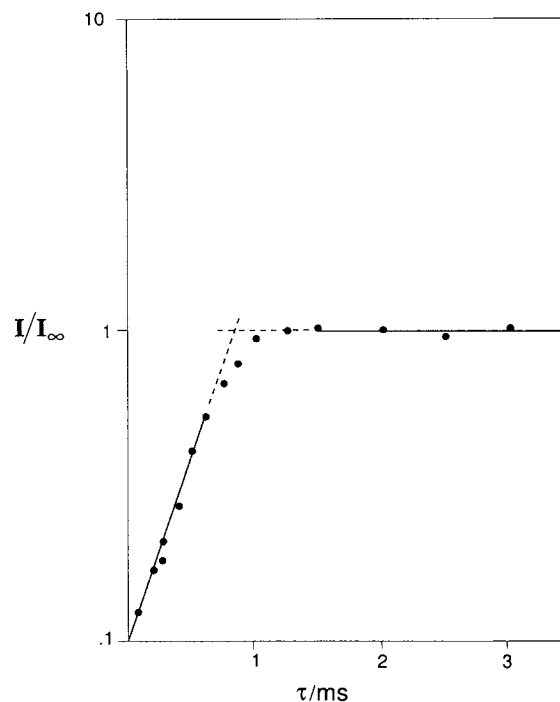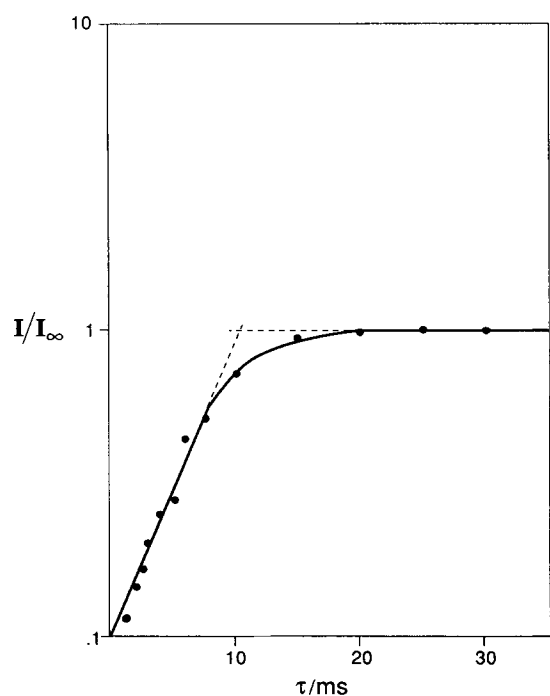

Figure 6 NMR spin diffusion times for the graft-co-polymer 49-1.

of the individually dispersed stiff chains is in agreement with NMR relaxation studies[49] and other observations[35] on rigid networks and gels. Com-

puter-aided molecular modeling also indicated an unexpected measure of flexibility of the stiff polyamide chains when these are in dilute solution or
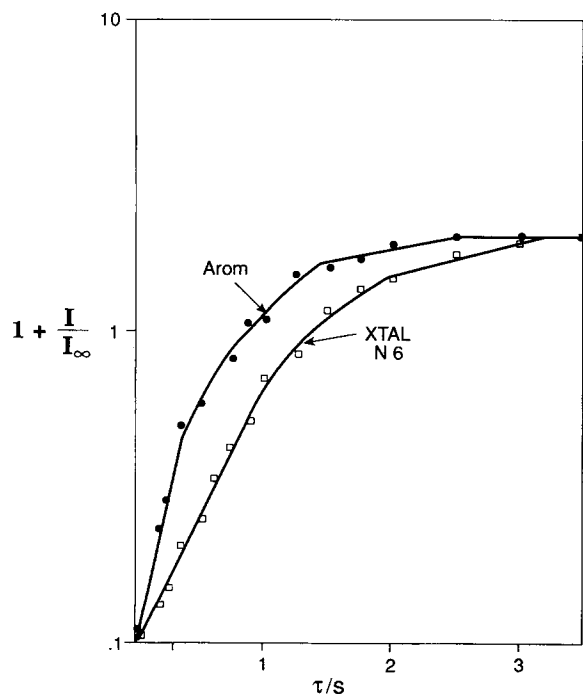
Figure 5 T_{1H} relaxation plot for the nylon 6 and polyamide 25A in the ungrafted blend 49-6.

Figure 7 NMR spin diffusion times for the ungrafted blend 49-6.

**Table II   Tensile Properties of Series 49 and 58**

Sample Code	Tensile Modulus (GPa)	Yield Stress (MPa)	Tensile Stress (MPa)	Breaking Strain (%)
49-1	1.55	39.1	45.9	61
49-2	1.42	37.6	59.0	119
49-3	1.16	32.6	53.6	166
49-4	0.96	30.5	56.9	234
49-5	0.82	28.0	48.0	252
49-6	1.04	32.0	51.1	148
58-1	1.50	42.4	61.1	129
58-2	1.29	38.5	62.1	171
58-3	1.10	34.8	62.9	215
58-4	0.94	32.5	60.0	238
58-5	0.79	27.6	48.9	252

All samples were dissolved in conc. sulfuric acid and precipitated in ice-water mixture prior to filtration, purification, drying, and molding. All tensile specimens were prepared, equilibrated at 50% relative humidity, and tested under identical conditions.

individually dispersed in the melt of flexible-chain polymers.[50,51]

The flexibility of the individual stiff aromatic chains in the graft-copolymers imparts to them worm-like and not rod-like behavior. Light scattering studies performed by many authors on dilute solutions of stiff polyamides similar to the present ones[52-55] lead to a concensus that the persistence
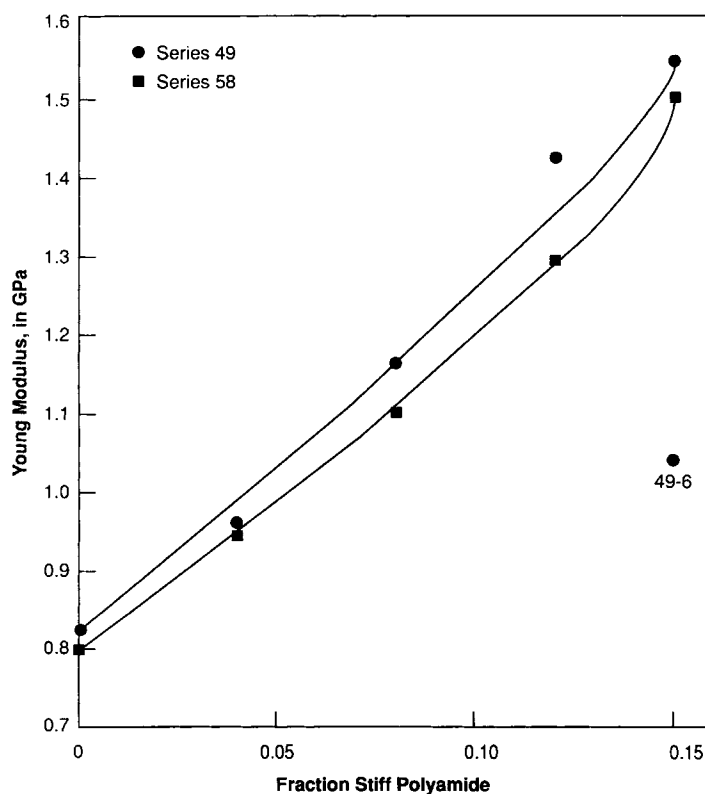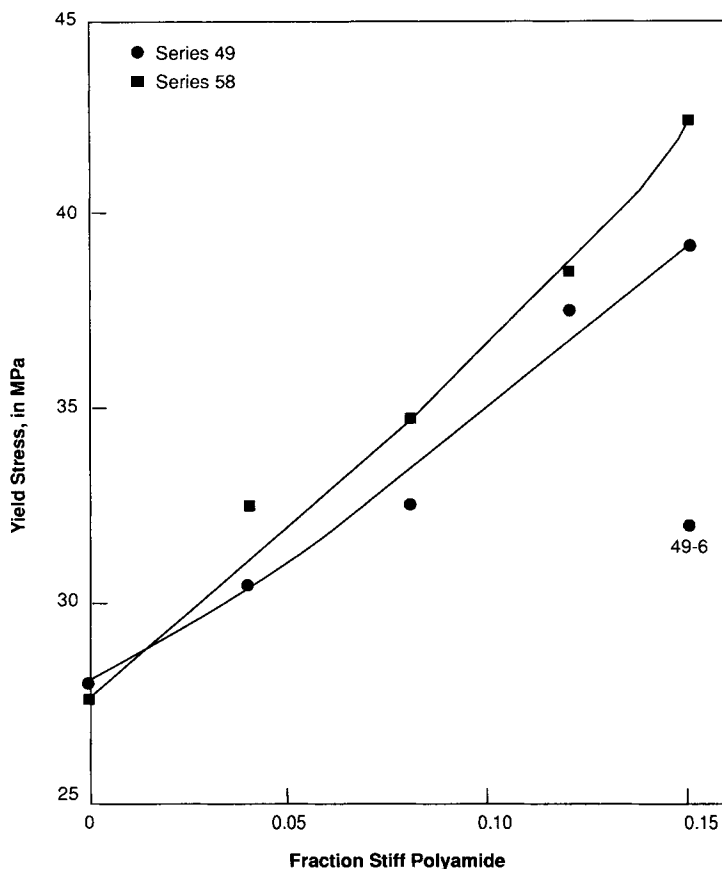

Figure 8   Tensile modulus of series 49 and 58 as a function of stiff polyamide concentration. Note the position of the ungrafted blend 49-6.

length, q, of stiff aromatic polyamide chains is on the order of 300 Å. Such a persistence length, corresponding to the length of no more than 50 aromatic repeat units, is a clear indication that the stiff polyamide chains are worm-like in character and are endowed with a substantial degree of flexibility. We believe that this flexibility is mirrored in the magnitude of the contribution of the stiff polyamide chains to the tensile properties of the graft-copolyamides and their blends with nylon 6.

Tensile tests were performed on low crystallinity specimens obtained by molding with QQ and subsequent equilibration at 50% RH. The amount of moisture pick-up during equilibration was the same within experimental error, reaching a total of 2.8 ± 0.1 wt % for each sample. Before proceeding further, we wish to stress that because the test specimens and the stiff chains in them are both unoriented, the level of reinforcement is expected to be substantially lower than in cases where either the reinforcing chains or the specimen as a whole are oriented in the test direction. The numerical test results are shown in Table II. To clarify the rela-

tionships between composition and tensile properties, and to ease the comparison between series 49 and 58, the Young's (tensile) modulus, yield stress, and breaking strain are plotted as functions of composition in Figures 8, 9 and 10, respectively. The tensile (breaking) stress values of series 49 were too scattered to be compared with those of series 58. The tensile stress results in Table II are given, hence, for the sake of completeness only and will not be discussed further. From Figure 8 we see that the Young's modulus values of members of series 49 are consistently somewhat higher than those of members of series 58 of the same composition. This, we believe, is due to the higher level of grafting achieved in series 49. The fact that the pure nylon 6 in series 49 shows slightly higher modulus than the pure nylon 6 of series 58 may, however, tell us that slight unaccounted differences in sample preparation of the two series may contribute part of the difference in modulus. The huge difference between the graft-copolymers 49-1 and 58-1 and the ungrafted blend 49-6, all of which contain 15% stiff polyamides and 85% nylon 6, is far larger than any potential exper-

Figure 9   Yield stress of series 49 and 58 as function of stiff chain concentration. Note the relative position of the ungrafted blend 49-6.
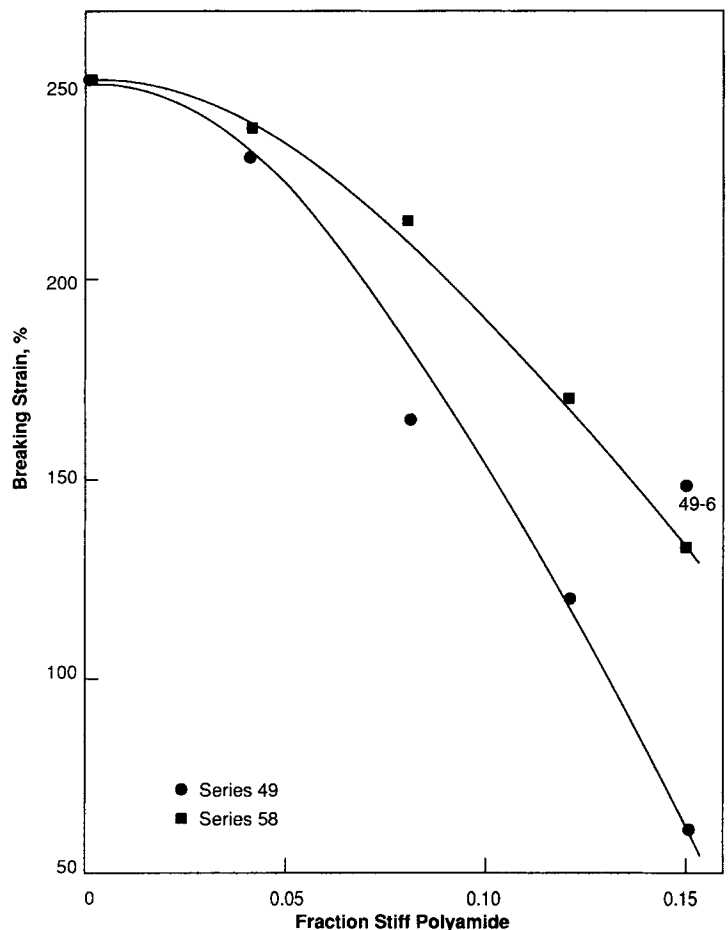
Figure 10   Breaking strain of series 49 and 58 as function of stiff chain concentration. Note position of ungrafted blend 49-6.
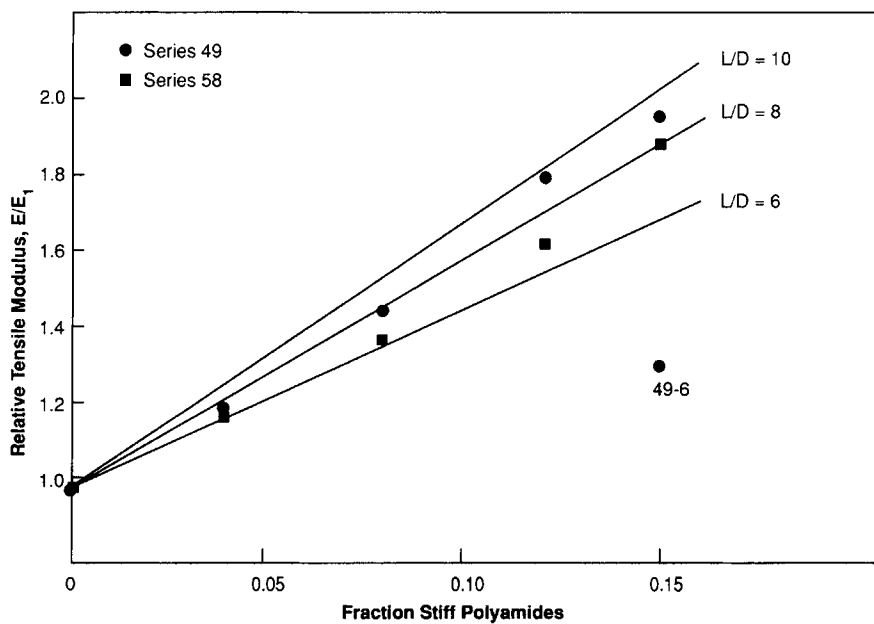
Figure 11   Relative tensile modulus plotted against fraction of stiff polyamide in series 49 and 58.

imental scatter. The relatively low modulus of 49-6 instructs us that the small aggregates of stiff polyamide blended in nylon 6 without grafting, contribute to modulus enhancement only a fraction of the contribution when the same amount of stiff polyamide is grafted to the nylon 6 and molecularly dispersed in it. The yield stress is plotted in Figure 9 against composition. The pattern is generally similar to the modulus results in Figure 8, except that in series 58 the yield stress is higher than in series 49. The blend 49-6 again shows much lower stress value than the compositionally identical graft-copolymers 49-1 and 58-1. In Figure 10 we see that the breaking strain drops precipituously with concentration of stiff polyamide in series 49 and less so in series 58. The drop is even smaller in the blend 49-6. We explain the above by the graft level in 49-1 and the blends 49-2, 49-3, and 49-4, is higher than for the corresponding members of series 58. This reduces the deformability under stress of series 49-1 through 49-4, relative to the corresponding members of series 58. Therefore, with increased strain on the specimens, more and larger microscopic zones of inhomogeneity appear in series 49 than in series 58, leading to reduced yield stress and catastrophic sample failure at lower strains.

There exists in the literature a simple rule of mixtures[56,57] describing the tensile modulus, E, of a reinforced composite in terms of the moduli of the matrix polymer, E_1, and the highly aligned, long reinforcing fibers, E_2:

$$E = E_1\phi_1 + E_2\phi_2 \qquad (1)$$

where ϕ_1 and ϕ_2 are the respective volume fractions of the matrix polymer and the reinforcing fibers. When the reinforcing phase is spherical in nature, then an inverse rule of mixtures applies:

$$1/E = \phi_1/E_1 + \phi_2/E_2. \qquad (2)$$

All experimental results obtained from our graft-copolymers and their blends with nylon 6 fell in between the results expected from Eqs. (1) and (2). On the other hand, an excellent agreement was found between the modulus of the ungrafted blend 49-6 and Eq. (2). Using E_1 and E_2 values to be discussed below, the modulus of 49-6 was calculated to be $E = 1.064$ GPa and the experimentally measured value was $E = 1.040$ GPa.

Because our experimental results fell in between Eqs. (1) and (2), it was felt that a relationship describing the behavior of randomly oriented reinforcement in polymeric composites may appropri-

ately describe our results. A scheme to handle this relationship was devised.[58–61] It allows the calculation of the tensile modulus of a composite relative to the modulus of the matrix material, provided the reinforcing particles are randomly dispersed in the system and the stresses transfer from the matrix to the reinforcement through the interfacial layer with no breakdown or delamination. For the calculations, the fractional volume of the two components must be known, together with the modulus of each and the axial ratio (L/D) of the reinforcing species. Alternatively, if the relative tensile modulus is known, then from the knowledge of all other parameters, the axial ratio of the reinforcing species may be calculated. For the nylon 6 matrix the modulus of E_1 = 0.8 GPa was used, averaging the close experimental results for 49-5 and 58-5 in Table II. The relatively low value of E_1 is due to the specimens being quick quenched, that is, substantially amorphous and unoriented, and fully equilibrated at 50% RH. For the stiff chain aromatic polyamide reinforcement, the modulus of Pp-PT was used. The value of E_2 = 112 GPa used by us was obtained by averaging the first six experimental and pertinent results in table 3 of the review article by Northolt and Sikkema.[62] Because our system was not annealed and oriented to enhance the crystallinity of the stiff polyamide component, it was felt that the use of the crystalline modulus of Pp-PT, about 153 GPa,[1] is not justified in our case. The equations used for the Halpin and Tsai procedure are:

$$E/E_1 = (1 + AB \cdot \phi_2)/(1 - B \cdot \phi_2 \cdot \Psi) \qquad (3)$$

and

$$B = [(E_2/E_1) - 1]/[(E_2/E_1) + A]. \qquad (4)$$

Here, A is a shape-dependent coefficient related to the axial ratio L/D of the reinforcing species[61] and Ψ is defined by

$$\Psi = 1 + [(1 - \phi_m)/\phi_m^2]\phi_2 \qquad (5)$$

where ϕ_m is the maximum value of the packing fraction of randomly oriented fibers, assumed to be ϕ_m = 0.82.[9] In our case, Ψ increases from 1.00 to 1.04 as ϕ_2 goes from 0 to 0.15. The relative modulus E/E_1 is plotted in Figure 11 against the weight fraction of stiff polyamides for series 49 and 58. The very low value of E/E_1 for the blend 49-6 clearly indicates the relatively low reinforcement of the ungrafted, blended stiff polyamide. This lower performance may be caused by agglomeration of the reinforcing

species, poor adhesion between the reinforcement and the matrix, or both.

The Halpin–Tsai results in Figure 11 are consistent with the axial ratio of the reinforcing stiff molecules in the graft-copolymers being in the range of $6 < L/D < 10$. This corresponds to lengths of 40–65 Å and to stiff chain molecular weight of 720 $< M_n < 1200$. The low M_n values imply that for the purpose of reinforcing, each stiff worm-like chain behaves as a series of short rod–like entities connected to one another by flexible decoupling joints.

Throughout our calculations, the ratio of E_2/E_1 = 140 was used in the determination of the parameter B in Eqs. (3) and (4). It is interesting to note that if the ratio of E_2/E_1 becomes smaller, the resulting data points in plots of E/E_1 vs. ϕ_2 maintain their scatter and the curves drawn through them keep practically the same slopes as in Figure 11. What does change is the axial ratio associated with each curve. Thus, when values of E_1 = 20 GPa, E_2 = 153 GPa, and E_2/E_1 = 7.5 were used, values of L/D = 45, 25, and 15 were obtained for the three curves in Figure 11. This indicates that in order to determine a correct L/D ratio, accurate values of E_1 and E_2 must be used.

REFERENCES

1. K. Tashiro, M. Kobayashi, and H. Tadokoro, *Macromolecules*, **10**, 413 (1977).
2. P. J. Flory, *Macromolecules*, **11**, 1138 (1978).
3. S. M. Aharoni, *Polymer*, **21**, 21 (1980).
4. O. Olabisi, L. M. Robeson, and M. T. Shaw, *Polymer-Polymer Miscibility*. Academic Press, New York, 1979.
5. M. M. Coleman, J. F. Graf, and P. C. Painter, *Specific Interactions and the Miscibility of Polymer Blends*. Technomic Publishing Co., Lancaster PA, 1991.
6. T. S. Ellis, *Macromolecules*, **22**, 742 (1989).
7. T. S. Ellis, *Polym. Eng. Sci.*, **30**, 998 (1990).
8. D. W. Van Krevelen, *Properties of Polymers*, Elsevier, Amsterdam, 1990, pp. 227–241, 493–494.
9. M. Takayanagi, T. Ogata, M. Morikawa, and T. Kai, *J. Macromol. Sci. Phys.*, **B17**, 591 (1980).
10. T. Oono, F. Kumamaru, T. Kajiyama, and M. Takayanagi, *Rep. Prog. Polym. Phys. Jpn.*, **24**, 193 (1981).
11. M. Takayanagi, T. Kajiyama, and T. Katayose, *J. Appl. Polym. Sci.*, **27**, 3903 (1982).
12. M. Takayanagi and T. Katayose, *Polym. Eng. Sci.*, **24**, 1047 (1984).
13. A. Ye Chalykh, V. P. Dmitrenko, G. S. Golovkin, and A. Ye Rubtsov, *Polym. Sci. USSR*, **31**, 2168 (1989).
14. T. Kyu, T. I. Chen, H.-S. Park, and J. L. White, *J. Appl. Polym. Sci.*, **37**, 201 (1989).
15. T. I. Chen and T. Kyu, *Polym. Commun.*, **31**, 111 (1990).
16. H. W. Kammer and C. Kummerlowe, *Acta Polymerica*, **41**, 269 (1990).
17. M. F. Lin and H.-H. Wang, *J. Mater. Sci. Lett.*, **10**, 569 (1991).
18. D. Beery, S. Kenig, and A. Siegmann, *Polym. Eng. Sci.*, **31**, 451, 459 (1991).
19. H.-H. Wang and M.-F. Lin, *J. Appl. Polym. Sci.*, **43**, 259 (1991).
20. J.-C. Yang, T. Fukai, and T. Kyu, *Polym. Eng. Sci.*, **31**, 699 (1991).
21. M. Takayanagi and T. Katayose, *J. Polym. Sci., Polym. Chem. Ed.*, **19**, 1133 (1981).
22. M. Takayanagi, S. Ueta, W. Y. Lei, and K. Koga, *Polym. J.*, **19**, 467 (1987).
23. M.-L. Chen, S. Ueta, and M. Takayanagi, *Polym. J.*, **20**, 673 (1988).
24. F. P. M. Mercx and P. J. Lemstra, *Polym. Commun.*, **31**, 252 (1990).
25. R. R. Burch, W. Sweeny, H.-W. Schmidt, and Y. H. Kim, *Macromolecules*, **23**, 1065 (1990).
26. R. R. Burch and L. E. Manring, *Macromolecules*, **24**, 1731 (1991).
27. Y. Wu and G. D. Tesoro, *J. Appl. Polym. Sci.*, **31**, 1041 (1986).
28. M. Breznick, J. Banbaji, H. Guttmann, and G. Marom, *Polym. Commun.*, **28**, 55 (1987).
29. G. C. Tesoro, R. Benrashid, L. Rebenfeld, and U. Gaur, Int. Symp. Polym. Adv. Technol. Invited Lectures and Selected Contributed Papers, M. Lewin, Ed., VCH, New York, 1988, pp. 773–791.
30. S. Erhan, U.S. Pat. 4,845,278 (July 1989).
31. A. E. Hoyt and B. C. Benicewicz, *J. Polym. Sci. A, Polym. Chem.*, **28**, 3403 (1990).
32. D. R. Moore and L. J. Mathias, *J. Appl. Polym. Sci.*, **32**, 6299 (1986).
33. H. W. Spiess, *Chem. Rev.*, **91**, 1321 (1991).
34. J. Clauss, K. Schmidt-Rohr, and H. W. Spiess, *Acta Polym.*, **44**, 1 (1993).
35. S. M. Aharoni, *Macromolecules*, **24**, 4286 (1991).
36. N. Yamazaki, M. Matsumoto, and F. Higashi, *J. Polym. Sci., Polym. Chem. Ed.*, **13**, 1373 (1975).
37. S. M. Aharoni, *Macromolecules*, **15**, 1311 (1982).
38. S. M. Aharoni, *Macromolecules*, **20**, 2010 (1987).
39. G. Weill, *J. Macromol. Sci. Chem.*, **A27**, 1769 (1990).
40. S. A. Curran and S. M. Aharoni, AlliedSignal Inc. Research Report 91-36 of September 1991, to appear.
41. D. G. Cory and W. M. Ritchey, *Macromolecules*, **22**, 1611 (1989).
42. A. Pines, M. Gibby, and J. S. Waugh, *J. Chem. Phys.*, **59**, 569 (1973).
43. D. E. Axelson, *High Resolution NMR Spectroscopy of Polymers in Bulk*, R. A. Komoroski, Ed., VCH Publishers, 1986, pp. 191–193.
44. M. G. Columbo, B. H. Meier, and R. R. Ernst, *Chem. Phys. Lett.*, **146**, 189 (1988).
45. S. A. Curran and A. R. Padwa, *Macromolecules*, **20**, 625 (1987).
46. E. O. Stejskal, J. Schaefer, M. D. Sefcik, and R. A. McKay, *Macromolecules*, **14**, 275 (1981).

47. D. L. Vanderhart, *Makromol. Chem. Macromol. Symp.*, **34**, 125 (1990).

48. K. Schmidt-Rohr, J. Clauss, B. Blumich, and H. W. Spiess, *Magn. Reson. Chem.*, **28**, 53 (1990).

49. S. A. Curran, C. P. LaClair, and S. M. Aharoni, *Macromolecules*, **24**, 5903 (1991).

50. W. B. Hammond, S. M. Aharoni, and S. A. Curran, in *Synthesis, Characterization, and Theory of Polymeric Networks and Gels*, S. M. Aharoni, Ed., Plenum, New York, 1992, pp. 93–112.

51. A. R. Khokhlov, personal communication, August 1991.

52. K. Zero and S. M. Aharoni, *Macromolecules*, **20**, 1957 (1987).

53. M. Arpin and C. Strazielle, *Polymer*, **18**, 591 (1977).

54. Q. Ying and B. Chu, *Makromol. Chem. Rapid Commun.*, **5**, 785 (1984).

55. W. R. Krigbaum, T. Tanaka, G. Brelsford, and A. Cifferi, *Macromolecules*, **24**, 4142 (1991).

56. A. Kohli, N. Chung, and R. A. Weiss, *Polym. Eng. Sci.*, **29**, 573 (1989).

57. D. Dutta, H. Fruitwala, A. Kohli, and R. A. Weiss, *Polym. Eng. Sci.*, **30**, 1005 (1990).

58. J. C. Halpin, *J. Composite Mater.*, **3**, 732 (1969).

59. L. E. Nielsen, *J. Appl. Phys.*, **41**, 4626 (1970).

60. T. B. Lewis and L. E. Nielsen, *J. Appl. Polym. Sci.*, **14**, 1449 (1970).

61. L. E. Nielsen, *Mechanical Properties of Polymers and Composites*, Vol. 2, Marcel Dekker, New York, 1974, Chap. 7 and 8.

62. M. G. Northolt and D. J. Sikkema, *Adv. Polym. Sci.*, **98**, 115 (1990).